BULLETIN OF THE EARTHQUAKE
RESEARCH INSTITUTE
Vol. 44 (1966), pp. 609-643

35. *Comparative Studies of Earthquake Motions on the Ground and Underground. II.*

By Kiyoshi KANAI, Teiji TANAKA,
Shizuyo YOSHIZAWA, Toshizo MORISHITA,
Kaio OSADA and Tomisaburo SUZUKI,

Earthquake Research Institute.

(Read Nov. 24, 1964 and Mar. 22, 1966.—Received Mar. 31, 1966.)

1. Introduction

It has been proved by many authors, in general, that the amplitudes of earthquake motions underground are smaller than those on the ground and that the shorter the period of earthquake motions is, the smaller the ratio of the amplitudes underground to those on the ground.

Recently, from the results of the comparative observations of earthquake motions, both on the ground and in the depths of the earth, it was found that the distribution of the amplitudes of earthquake motions as to the depths in the earth is not as simple as was considered formerly. Further, it was proved both by observation and theory that the modifications of earthquake motions of moderate epicentral distance in ground may be considered as the multiple reflection phenomena of the elastic waves in a surface layer.[1)]

In the present paper we are, firstly, going to carry out the mathematical examinations by a new method[2)] based on the theory of the multiple reflections of seismic waves in a superficial layer. Secondly, one of the empirical formulae for the spectrum of earthquake motions obtained in the previous paper[3)] is improved somewhat.

---

1) R. TAKAHASI and K. HIRANO, "Seismic Vibrations of Soft Ground," *Bull. Earthq. Res. Inst.*, **19** (1941), 544-548 (in Japanese).

K. KANAI, T. TANAKA and S. YOSHIZAWA, "Comparative Studies of Earthquake Motions on the Ground and Underground," *ditto*, **37** (1959), 53-87.

E. SHIMA, "Modifications of Seismic Waves in Superficial Soil Layers as Verified by Comparative Observations on and beneath the Surface," *ditto*, **40** (1962), 187-259.

2) K. KANAI and S. YOSHIZAWA, "Some New Problems of Seismic Vibrations of a Structure. Part 1," *ditto*, **41** (1963), 825-833.

3) K. KANAI, "An Empirical Formula for the Spectrum of Strong Earthquake Motions," *ditto*, **39** (1961), 85-89.

2. Simultaneous observations of earthquake motions

The stations where the simultaneous observations of earthquake motions on the surface and in the depths of the earth were made, namely,

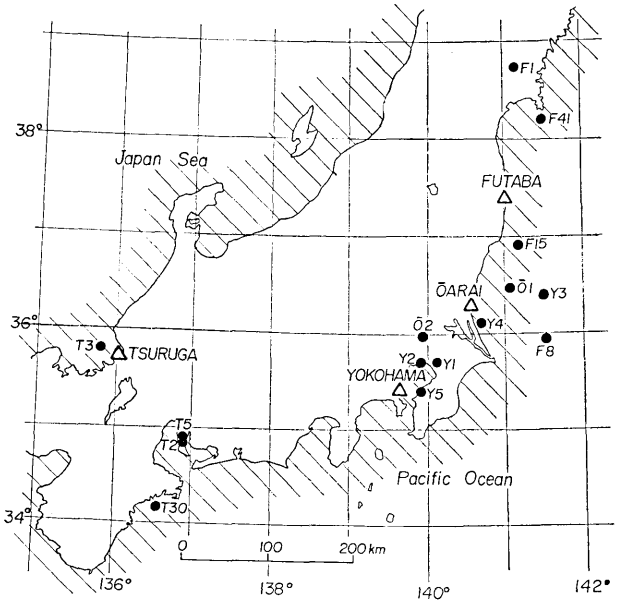

Fig. 1. Location of the observation stations and the epicenters of the earthquakes.

Table 1. Location of the observation stations.

Station	Location		Period of obs.	Observation Point	
	Longitude	Latitude			Depth (m)
Tsuruga	136.02	35.75	Aug. 1963~May 1964	A	0, 8.3
				B	0, 17.4, 36.8
Ōarai	140.50	36.27	Feb. 1965~June 1965	A	0, 12.7, 22.2
				B	0, 7.6, 14.7
Futaba	141.03	37.42	May 1965~Dec. 1965	A	0, 20.2, 52.4
				B	0, 20.8
Yokohama	139.63	35.38	Aug. 1965~Jan. 1966		0, 12.0, 37.3

Tsuruga, Ōarai, Futaba and Yokohama, are represented in Fig. 1 as well as Table 1.

Next, the instrumentation and the method of analysis used in the present investigations will be briefly described.

A six-channel electromagnetic seismometer with a photographic recording system was used. The seismometer consists of bore-hole geophones, ultra-low frequency amplifiers and an electromagnetic oscillograph. The geophones were the so-called self-levelling type[4] having an inverted pendulum of one sec period and critically damped. A six-channel transistor amplifier with integrating circuit was newly constructed. As for the recorder the MR-102A type oscillograph equipped with six elements of the G-300A galvanometer, of which the resonant frequency is 300 c/s, was employed. As the seismometer is a combination of these, it acts as a displacement-meter in the period range from 0.05 sec to 0.8 sec. At the stations Ōarai and Futaba, the integrating circuits in the amplifier were so switched off that the obtained record is proportional to the ground velocity in the same period range.

In the present cases, a newly-built electric self-starter[5] and a time printer were used. When the oscillograph is triggered by an earthquake a 30-sec record is taken, its date and time being printed on a paper automatically. The paper speed and the time marks of the record were chosen to be 3 or 6 cm/sec and 1/10, 1/50 or 1/100 sec, respectively, according to the predominant period of the ground at each station. The seismometer constants and pertinent operating details are given in Table 2. The overall period response curves of the seismometers for the station Tsuruga are shown in Fig. 2 as an example.

Table 2. The constants of the seismometers.

Observation station	No. of geophones	Type of seismometer	Magnification or sensitivity (max.)	Paper speed (cm/sec)	Timing marks (sec)
Tsuruga	5	Displacement	1000	3	1/10
Ōarai	6	Velocity	145 (mm/kine)	6	1/100
Futaba	5	Velocity	350 (mm/kine)	6	1/100
Yokohama	3	Displacement	500	3, 6	1/50

4) K. KANAI and T. TANAKA, "Self-levelling Vibrograph," *Bull. Earthq. Res. Inst.*, **36** (1958), 359-368.

5) T. TANAKA, "A Starter for Observation of Earthquakes," *ditto*, **36** (1958), 465-470 (in Japanese).

At the stations, excepting Yokohama, the geophones were set at two points, 100–300 m distant from each other, where the subsoil conditions are somewhat different. Then the electrical outputs from the geophones at one point were led to the other by a shielded cable in order to record all seismograms on a single recording paper. Some examples of the seismograms are shown in Figs. 26 and 27.

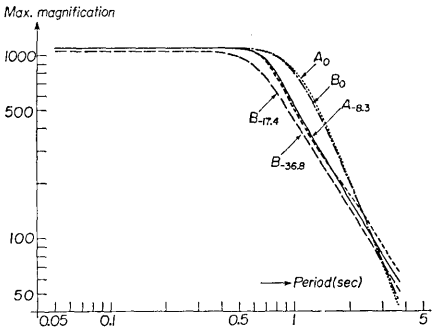

Fig. 2. An example of the period response curves of a 6-channel electromagnetic seismometer.

For the analysis, a 10 or 20 seconds portion was taken from a seismogram and amplitudes at every 1/50 or 1/100 sec were read with an accuracy of 0.1 mm. Consequently, 1000 or 2000 data points were taken in each seismogram. The calculation of the Fourier transform were made mostly by the IBM 7090 computer. The correction of the period characteristics of the seismometer was made for the amplitudes of the Fourier spectrum.

3. Results of the observations of earthquake motions

The positions of the seismometers installed together with the geological formations of the areas and subsoil conditions detected by boring at Tsuruga, Ōarai, Futaba and Yokohama are shown in Figs. 3–6. The dates as well as origins of the earthquakes treated in the present investigations are listed in Table 3.

The displacement or velocity spectra of earthquake motions were derived from the Fourier analysis of the records by means of the IBM 7090 computer. The velocity and acceleration spectra were calculated from the

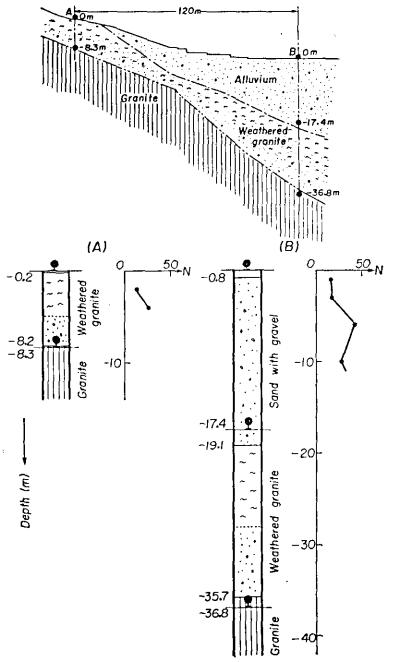

Fig. 3. Station Tsuruga. Geological formations and subsoil conditions.

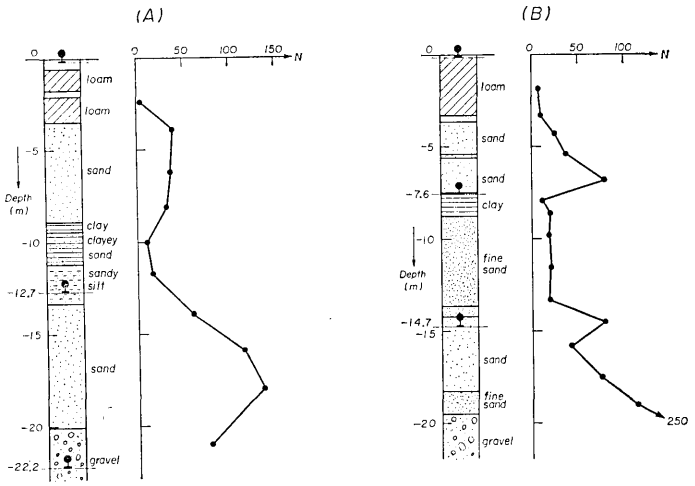

Fig. 4. Station Ōarai. Subsoil conditions.

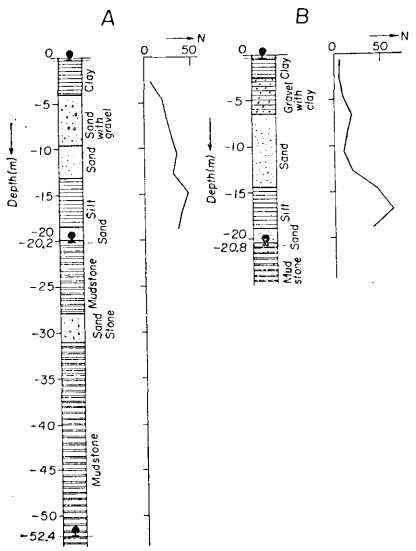

Fig. 5. Station Futaba. Subsoil conditions.

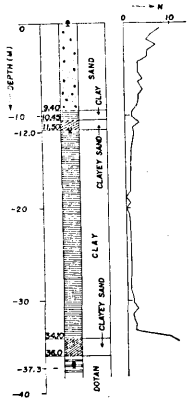

Fig. 6. Station Yokohama. Subsoil conditions.

Table 3. Data of the earthquakes treated here.

Station	No.	Date	Origin			M
			Longitude	Latitude	Depth (km)	
Tsuruga	T 2	1963 IX 4	136.9	34.9	0	4.2
	T 3	〃 〃 6	135.8	35.8	0	—
	T 5	〃 〃 17	136.9	34.9	0	4.1
	T 16	〃 X 26~30	—	—	—	—
	T 30	1964 II 4	136.6	34.2	60	5.3
Ōarai	O 1	1965 IV 12	141.1	36.5	40	4.6
	O 2	〃 〃 13	139.9	36.0	40	5.1
Futaba	F 1	〃 V 16	141.2	38.7	0	4.9
	F 8	〃 VI 8	141.5	35.9	20	4.7
	F 15	〃 〃 23	141.2	36.9	40	4.5
	F 20	〃 VII 3~ 4	—	—	—	—
	F 41	〃 VIII 14	141.5	38.2	20	—
	F 47	〃 VIII 24~25	—	—	—	—
	F 60	〃 IX 18~19	—	—	—	—
	F 67	〃 X 6~ 7	—	—	—	—
Yokohama	Y 1	〃 IV 3	140.1	35.7	80	—
	Y 2	〃 〃 〃	139.9	35.7	80	—
	Y 3	〃 〃 23	141.5	36.4	40	6.4
	Y 4	〃 X 4	140.7	36.1	60	—
	Y 5	〃 〃 23	139.9	35.4	70	—

displacement or velocity spectra on the assumption of simple harmonic motion. The velocity and acceleration spectra obtained here are shown in Figs. 28–31 and 32–35, respectively.

Roughly speaking, it will be seen from Figs. 28–31 that the velocity-period curve at depth takes a considerably flat form. A curve represented in Fig. 45 is the average of eight curves of Fig. 30 and it can be seen clearly in this figure that the velocity spectrum takes a considerably flat form. Therefore, it may be said still more conclusively that the seismic waves of considerably wide range of period in bed rock satisfy the nature of energy equipartition. That is to say, the amplitude-period relation of seismic waves in bed rock can be assumed as follows: $A/T=\text{constant}\,[(0.1-0.2\,\text{sec})<T<T_m]$, in which A, T and T_m, respectively, represent each amplitude and period of seismic waves and the period corresponding to the peak of displacement-period curve which is a function of magnitude.

It may be found from Figs. 28–35 that the amplitude of earthquake motion on the ground is larger than that in the depths of the ground. In order to make clearer the amplitude relation between the ground surface and underground, we calculated the amplitude ratios of the ground surface to the underground in each period from the results of spectral analysis which are shown in Figs. 28–31 or 32–35.

Further, the relations of the above-mentioned ratio to period at Tsuruga, Ōarai, Futaba and Yokohama are shown in Figs. 36–38, 39–40, 41–43 and 44.

The average curves of the amplitude ratio of the ground surface to the underground to period obtained from Figs. 36–44 are shown in Figs. 7–15.

Figs. 8a, 10a, 11a, 12a and 15a tell us that, in general, the amplitudes of earthquake motions on the grounds at Tsuruga B corresponding to the periods of 0.1–0.15 sec and 0.35 sec, Ōarai A of 0.1 sec and 0.2 sec, Ōarai B of 0.1 sec and 0.2 sec, Futaba A of 0.1 and 0.5 sec and Yokohama of 0.45–0.55 sec and 0.8–1.1 sec, that is, predominant periods of these grounds, grew considerably large.

The amplitudes of earthquake motions versus depth from the ground surface at each station obtained after the figures mentioned above are shown in Figs. 16–20a. Fig. 20b shows the amplitude distribution of the periods of 0.74–1.1 sec obtained directly from the records at Yokohama

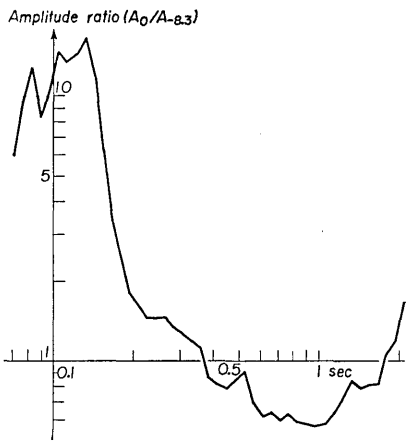

Fig. 7. Station Tsuruga A. Average of the amplitude ratios between the surface and 8.3 m depth.

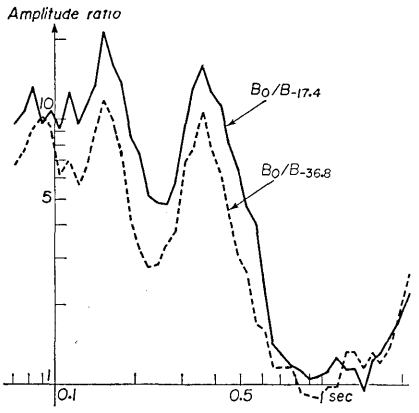

Fig. 8a. Station Tsuruga B. Average of the amplitude ratios between the surface and 17.4 m depth, and the surface and 36.8 m depth, respectively.

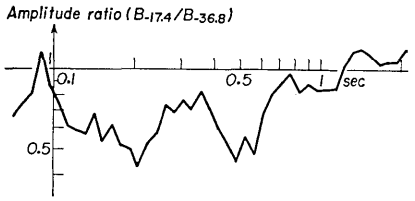

Fig. 8b. Station Tsuruga B. Average of the amplitude ratios between the 17.4 m depth and 36.8 m depth.

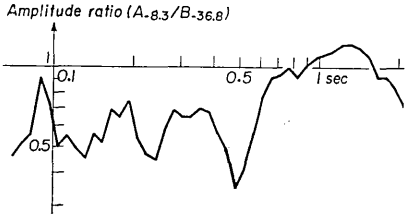

Fig. 9. Average of the amplitude ratios between the 8.3 m depth at A and 36.8 m depth at B of the station Tsuraga.

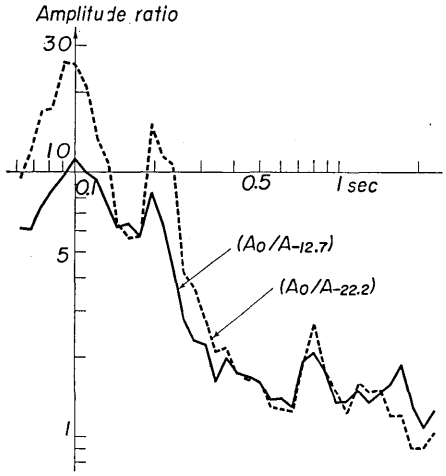

Fig. 10a. Station Ōarai A. Average of the amplitude ratios between the surface and 12.7 m depth, and the surface and 22.2 m depth, respectively.

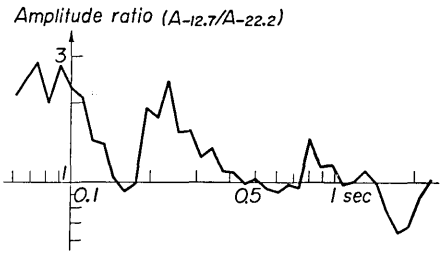

Fig. 10b. Station Ōarai A. Average of the amplitude ratios between 12.7 m depth and 22.2 m depth.

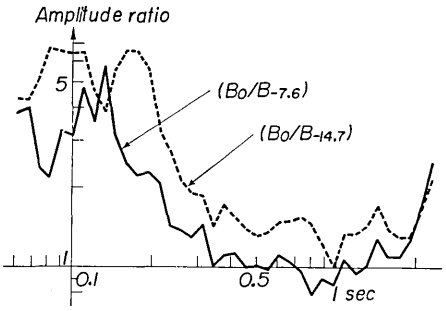

Fig. 11a. Station Ōarai B. Average of the amplitude ratios between the surface and 7.6 m depth, and the surface and 14.7 m depth, respectively.

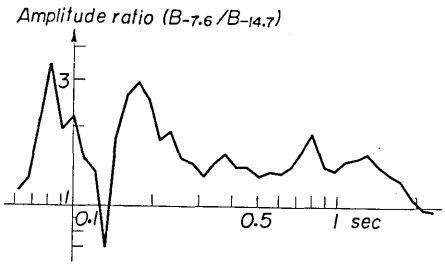

Fig. 11b. Station Ōarai B. Average of the amplitude ratios between 7.6 m depth and 14.7 m depth.

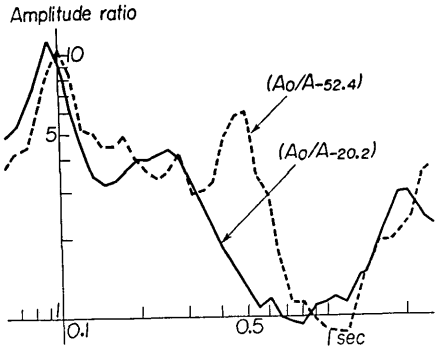

Fig. 12a. Station Futaba A. Average of the amplitude ratios between the surface and 52.4 m depth, and the surface and 20.2 m depth, respectively.

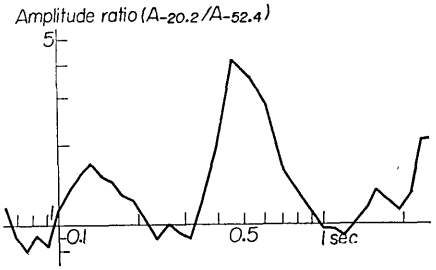

Fig. 12b. Station Futaba A. Average of the amplitude ratios between 20.2 m depth and 52.4 m depth.

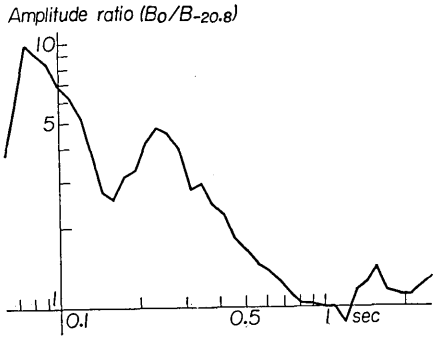

Fig. 13. Station Futaba B. Average of the amplitude ratios between the surface and the 20.8 m depth.

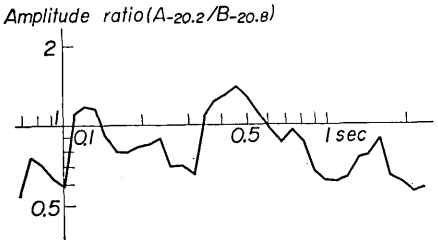

Fig. 14. Average of the amplitude ratios between 20.2 m depth at A and 20.8 m depth at B of the station Futaba.

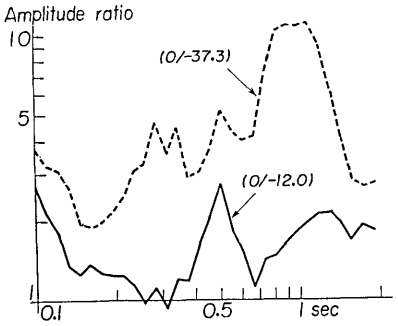

Fig. 15a. Station Yokohama. Average of the amplitude ratios between the surface and 37.3 m depth, and the surface and 12.0 m depth, respectively.

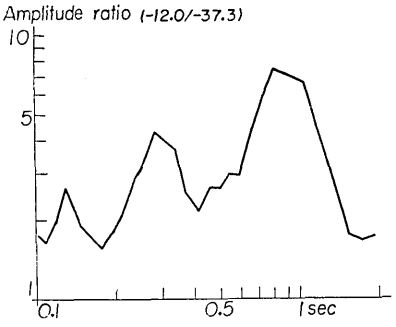

Fig. 15b. Station Yokohama. Average of the amplitude ratios between 12.0 m depth and 37.3 m depth.

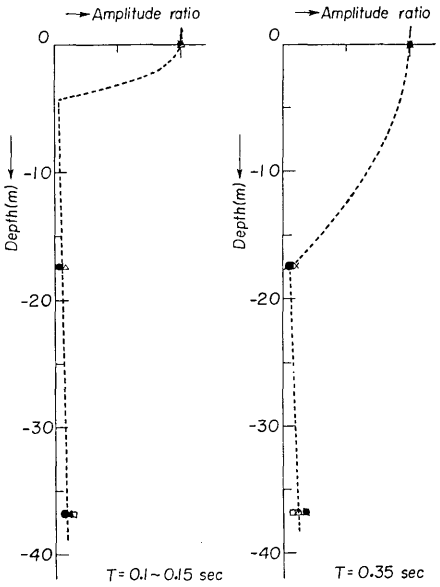

Fig. 16. Station Tsuruga B. Spectral amplitude of earthquake motions versus depth.

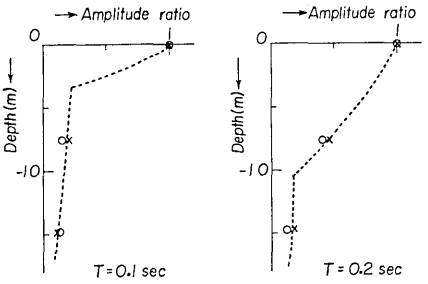

Fig. 18. Station Ōarai B. Spectral amplitude of earthquake motions versus depth.

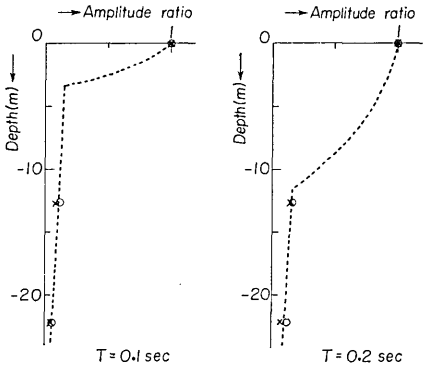

Fig. 17. Station Ōarai A. Spectral amplitude of earthquake motions versus depth.

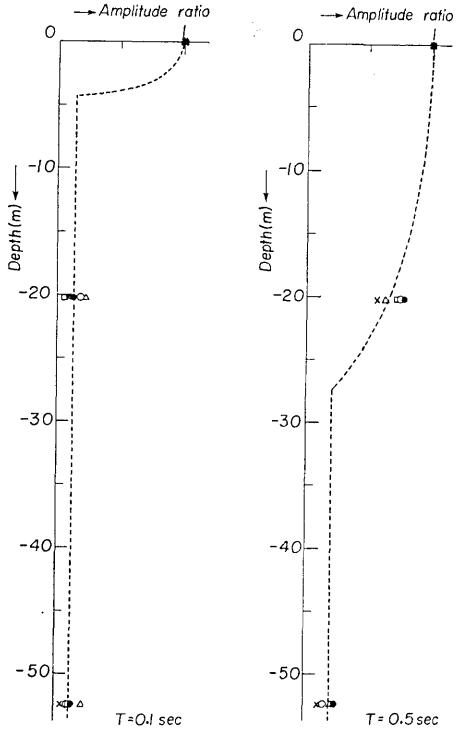

Fig. 19. Station Futaba A. Spectral amplitude of earthquake motions versus depth.

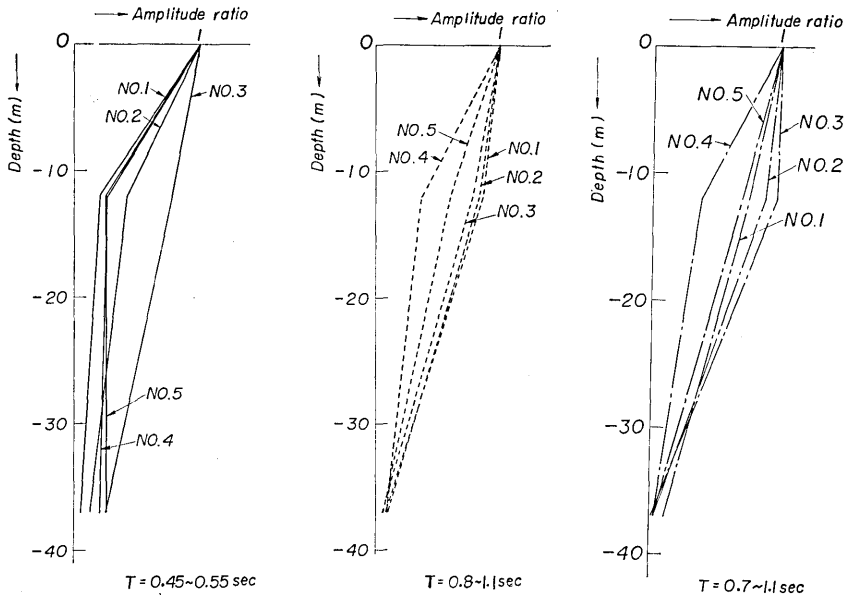

Fig. 20a. Station Yokohama. Spectral amplitude of earthquake motions versus depth.

Fig. 20b. Station Yokohama. Recorded amplitude of earthquake motions versus depth.

which is quite similar to the result shown in Fig. 20a.

The curves shown in Figs. 16-20b seem to be similar to the amplitude-depth distribution curve of a body having a double surface layer.

4. Multiple reflection problem

In this chapter, we will try to interpret the present observational results by the theory of multiple reflections of seismic waves in an elastic layer.

If the incident waves arriving at the lower boundary of a superficial layer of ground, $z=0$, be of the type;

$$u_0=F(t)\,, \tag{1}$$

the expression for the resulting motions at the surface, $z=H$, and the lower boundary, $z=0$, as influenced by the multiple reflections of seismic waves in that layer can be written by an infinite series, as follows;

$$U_{z=0}(t)=\gamma F(t)+\left\{\gamma F\left(t-\frac{2H}{V_1}\right)-\gamma\beta F\left(t-\frac{2H}{V_1}\right)\right\}+\cdots\,, \tag{2}$$

$$U_{z=H}(\tau)=2\gamma F\left(t-\frac{H}{V_1}\right)+2\gamma\beta F\left(t-\frac{3H}{V_1}\right)+\cdots, \tag{3}$$

in which $\beta=(\alpha-1)/(\alpha+1)$, $\gamma=2/(\alpha+1)$ and $\alpha=\rho_1V_1/\rho_2V_2$ and ρ_1, ρ_2, V_1, V_2 are the densities and the velocities of the superficial layer and the next lower layer, respectively, and $\tau=t-H/V_1$ and $\tau=0$ and $t=0$ correspond to the arrival time of seismic waves at $z=H$ and $z=0$, respectively.

From (2) and (3), a simple relation between the resulting motions at the surface, $z=H$, and the bottom of the superficial layer, $z=0$, have been obtained as follows:[6]

$$U_{z=0}\left(t-\frac{H}{V_1}\right)=\frac{1}{2}\left\{U_{z=H}(\tau)+U_{z=H}\left(\tau-\frac{2H}{V_1}\right)\right\}. \tag{4}$$

Now, we try to apply this method to the results of the observations of actual earthquake motions at the four stations. For applying the method, the value of $2H/V_1$ in a superficial layer has to be known. In this case it is estimated from the predominant period, T_G, of earthquake motions obtained at the surface by using the relation $T_G=4H/V_1$.

The final results of the calculations in the cases of Tsuruga A, Ōarai B, Futaba A and Yokohama are illustrated in Figs. 21–23 and 24, respectively.

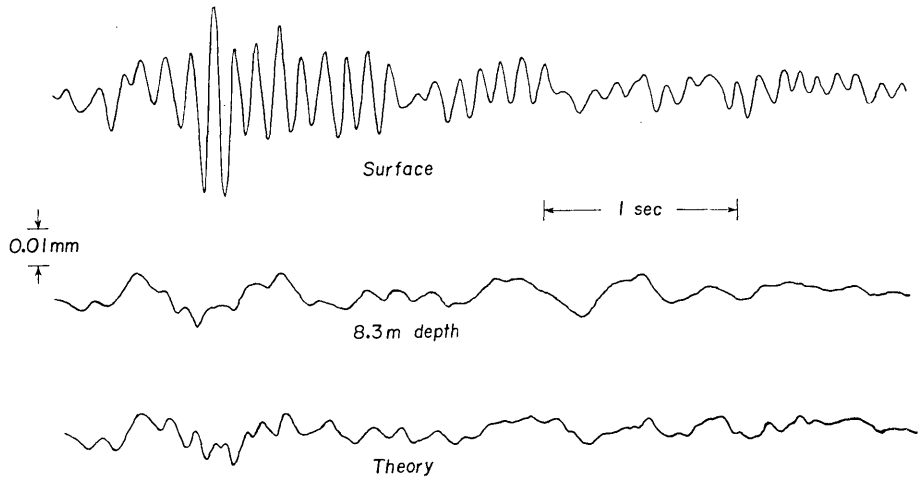

Fig. 21. Station Tsuruga. Seismograms observed at the surface and 8.3 m depth and the wave form at the bottom of the layer obtained theoretically.

6) *loc. cit.*, 2).

In these figures, the upper curves represent the actual records of earthquake motions at the surface and the middle and lower curves respectively are the actual records at the bottom of the superficial layer of the ground and the calculated wave forms at that bottom.

It will be seen in Figs. 21–24 that there is considerable agreement between the observational and theoretical results.

In other words, the present results tell us that the features of the earthquake motions in ground depend mostly on the multiple reflection phenomena of seimic waves.

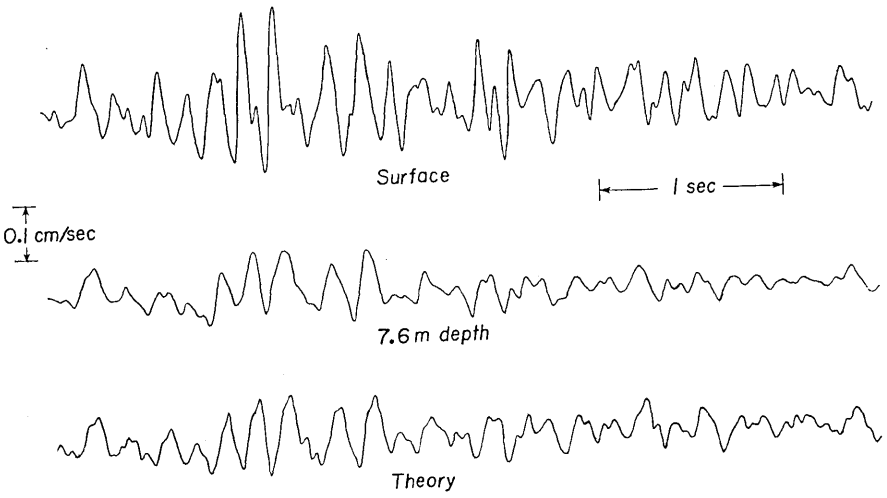

Fig. 22. Station Ōarai B. Seismograms observed at the surface and 7.6 m depth and the wave form at the bottom of the layer obtained theoretically.

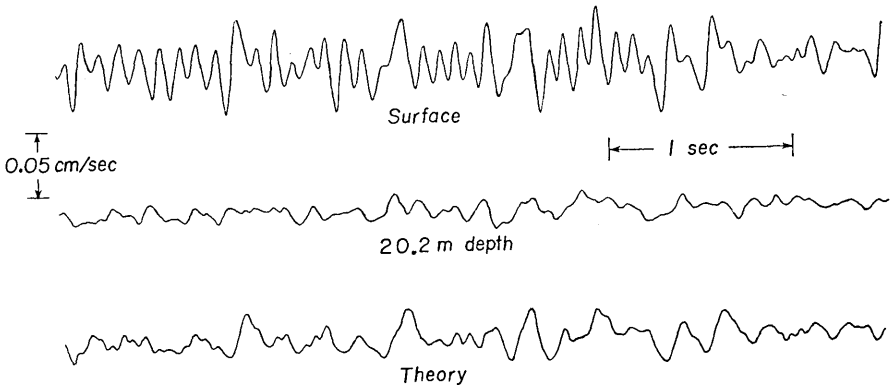

Fig. 23. Station Futaba A. Seismograms observed at the surface and 20.2 m depth and the wave form at the bottom of the layer obtained theoretically.

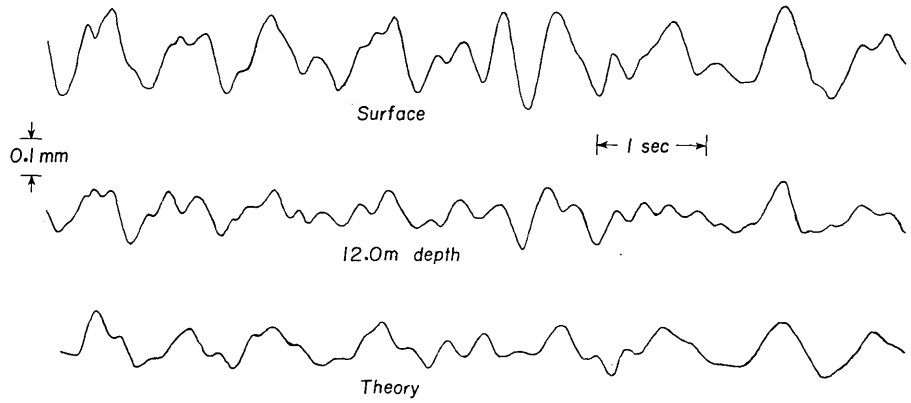

Fig. 24. Station Yokohama. Seismograms observed at the surface and 12.0 m depth and the wave form at the bottom of the layer obtained theoretically.

5. Velocity amplitude at bed rock

As we have seen in chapter 3 (see Fig. 45) that the velocity spectrum of the seismic waves at a deep depth satisfies the nature of energy equipartition, excepting considerably short periods and long periods of more than T_m mentioned previously.

The following empirical formula describes the value of velocity

Table 4. The calculated and observed maximum velocity amplitudes at bed rock.

Station	Earthq. No.	M	Hypocentral distance (km)	Max. velocity (cm/sec)	
				Calculated	Observed
Tsuruga	T 2	4.2±0.2	120	0.015~0.025	0.011
	T 5	4.1± 〃	120	0.012~0.021	0.022
	T 30	5.3± 〃	180	0.033~0.058	0.064
Ōarai	O 1	4.6± 〃	70	0.073~0.12	0.028
	O 2	5.1± 〃	80	0.11 ~0.20	0.19
Futaba	F 1	4.9± 〃	150	0.028~0.049	0.042
	F 8	4.7± 〃	170	0.017~0.030	0.033
	F 15	4.5± 〃	80	0.051~0.088	0.036
Yokohama	Y 3	6.4± 〃	220	0.13 ~0.22	0.21

amplitude of seismic waves at a deep depth of the hypocentral distance in km, R, and a magnitude, M:

$$v=10^{0.61M-1.73\log R-0.67} \qquad (5)$$

$$[0.05\sim 0.1\ \text{sec}<T<T_m]$$

in which

$$T_m=10^{0.39M-1.70}\,. \qquad (6)$$

The comparison between the values of velocity amplitude calculated by (5) and those obtained from the actual records is shown in Table 4 and Fig. 25. (The values of velocity amplitudes at Tsuruga and Yokohama were calculated numerically from the original displacement records

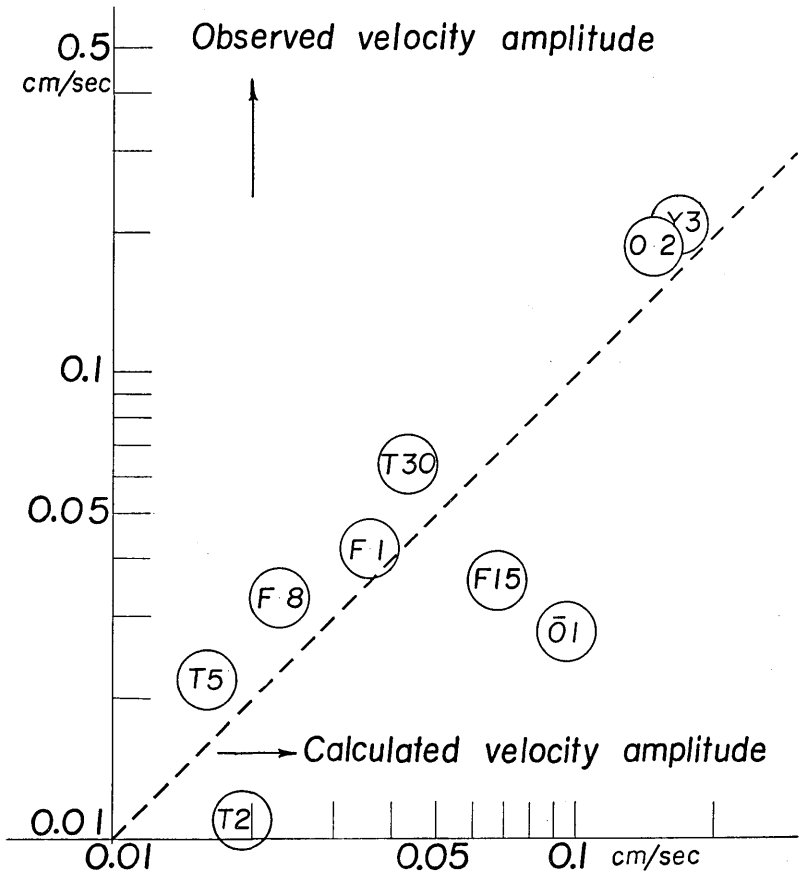

Fig. 25. Relation between the observed and calculated velocity amplitudes of earthquake motions at bed rock.

by means of the Lagrange's five point method. This calculation was made with the use of the HITAC 5020 computer in the University of Tokyo.) It will be seen in Table 4 as well as in Fig. 25 that the coincidence of the calculated and observed values is considerably good.

The present result tells us that equation (5) seems to be applicable in determining earthquake motions at bed rock for the purposes of structural design. The magnitudes and hypocentral distances of anticipated earthquakes may be estimated by the application of engineering judgment to statistical analyses of the seismicity.

The earthquake motions on the surface may be obtained by combining (5) with the following empirical formula, that is, the vibration characteristics of the ground:

$$G(T)=1+\frac{1}{\sqrt{\left[\frac{1+\alpha}{1-\alpha}\left\{1-\left(\frac{T}{T_G}\right)^2\right\}\right]^2+\left\{\frac{0.3}{\sqrt{T_G}}\left(\frac{T}{T_G}\right)\right\}^2}}, \tag{7}$$

in which α represents the impedance ratio of the ground to the bed rock and T_G is the predominant period of the ground.

6. Conclusion

From the present investigations, we ascertained more clearly that the features of the earthquake motions of a moderate hypocentral distance depend mostly on the multiple reflection phenomena of seismic waves in ground.

The present result tells us also that an empirical formula for the spectrum of strong earthquake motions may be applicable in determining earthquake ground motion characteristics for purposes of structural design.

In conclusion, we wish to express our sincere thanks to the Japan Atomic Power Co., Japan Atomic Energy Research Institute, Tokyo Electric Power Co., Inc. and Port and Harbor Bureau of Yokohama Municipal Office for their cooperation in the course of these investigations. A part of the computation in this study was carried out through the courtesy of the IBM, Japan Ltd. and the Computation Center, the University of Tokyo, to which our thanks are due. Our cordial thanks are also due to Misses K. Meguro and Y. Uemura who assisted in preparing this paper.

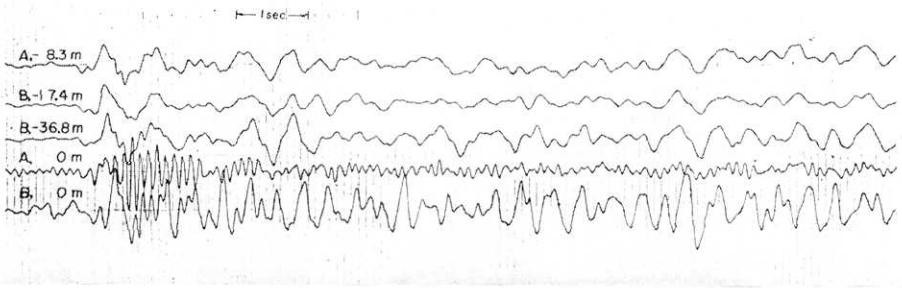

Fig. 26. An example of the seismograms obtained with the displacement type seismometer at the station Tsuruga (earthq. No. T16).

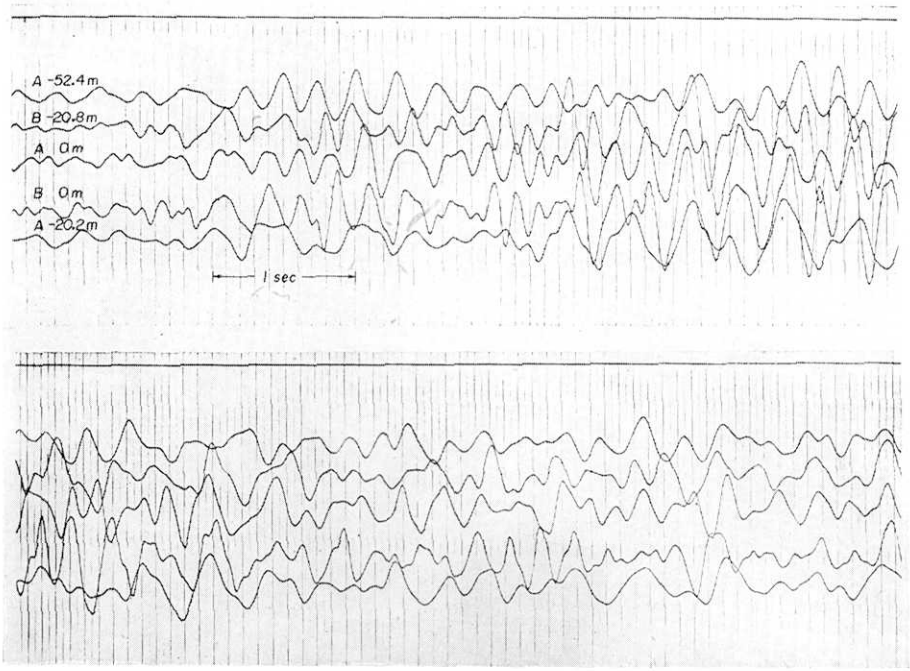

Fig. 27. An example of the seismograms obtained with the velocity type seismometer at the station Futaba (earthq. No. F60).

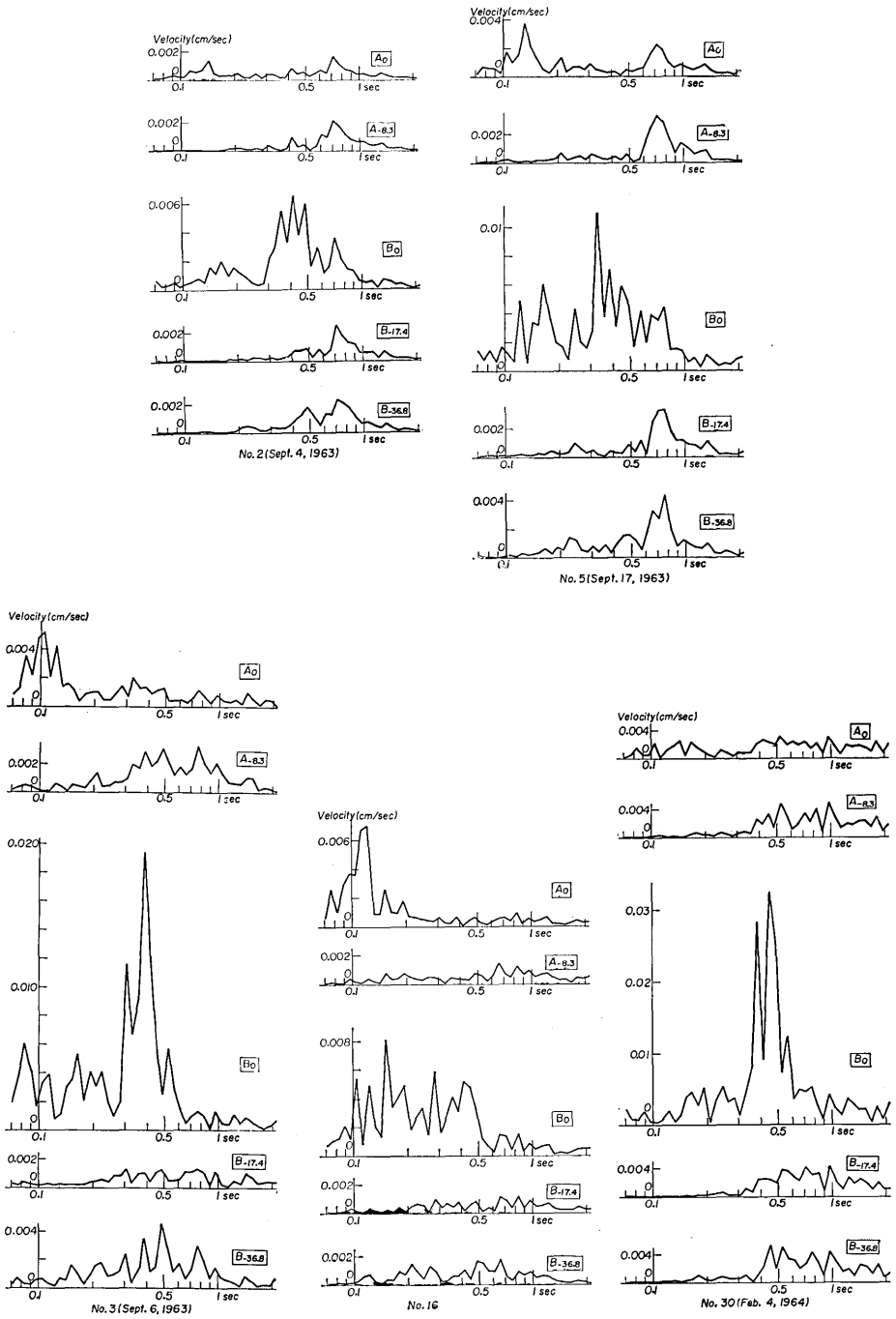

Fig. 28. Station Tsuruga. Velocity spectra of the earthquake motions.

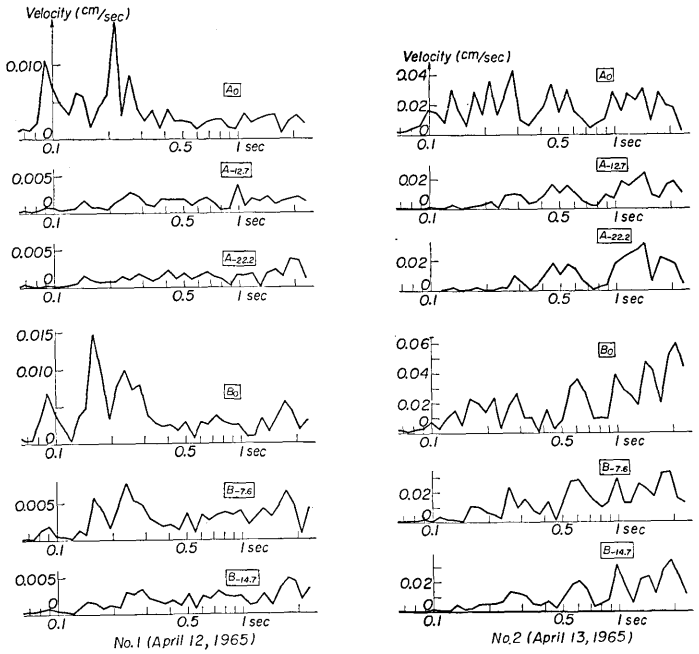

Fig. 29. Station Ōarai. Velocity spectra of the earthquake motions.

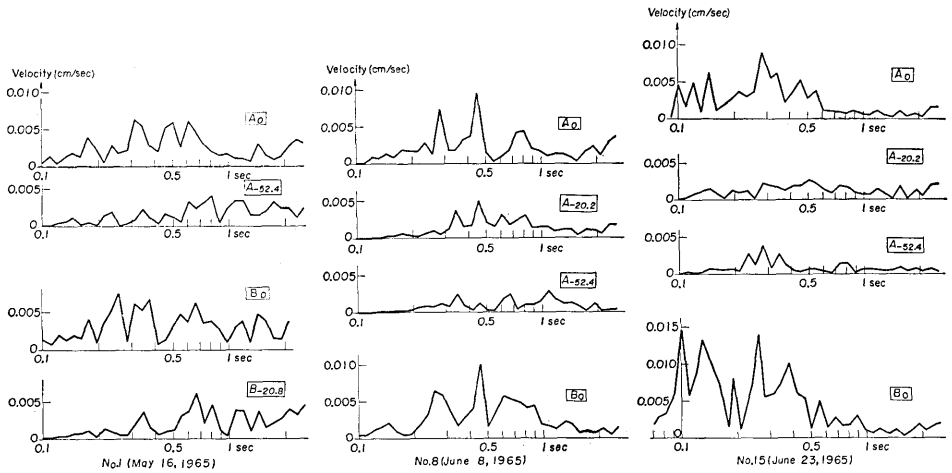

(to be continued)

(continued)

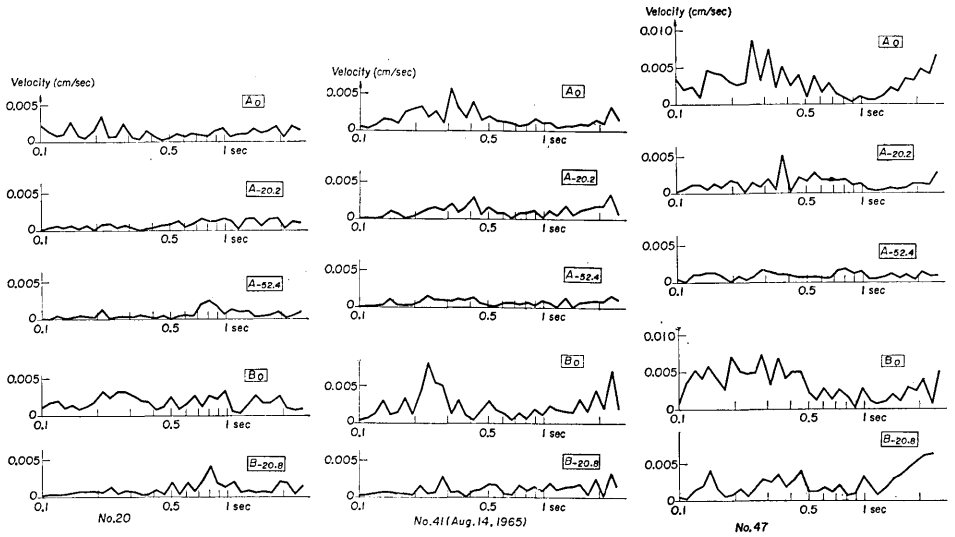

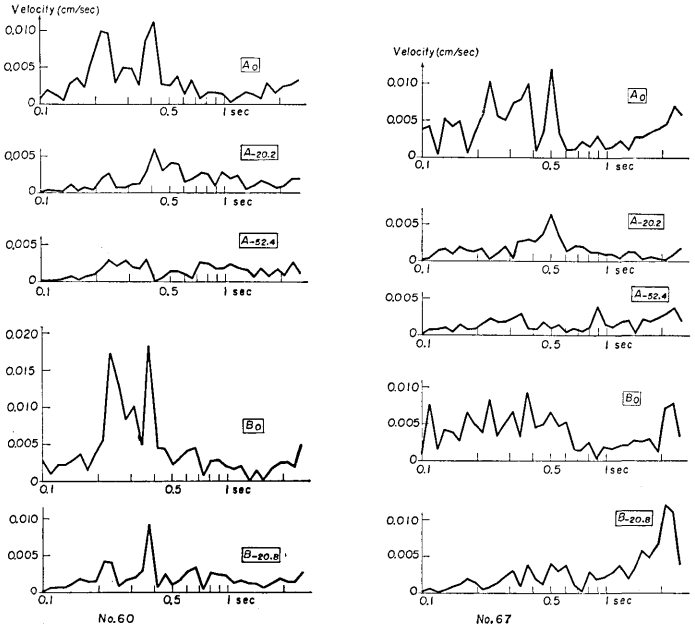

Fig. 30. Station Futaba. Velocity spectra of the earthquake motions.

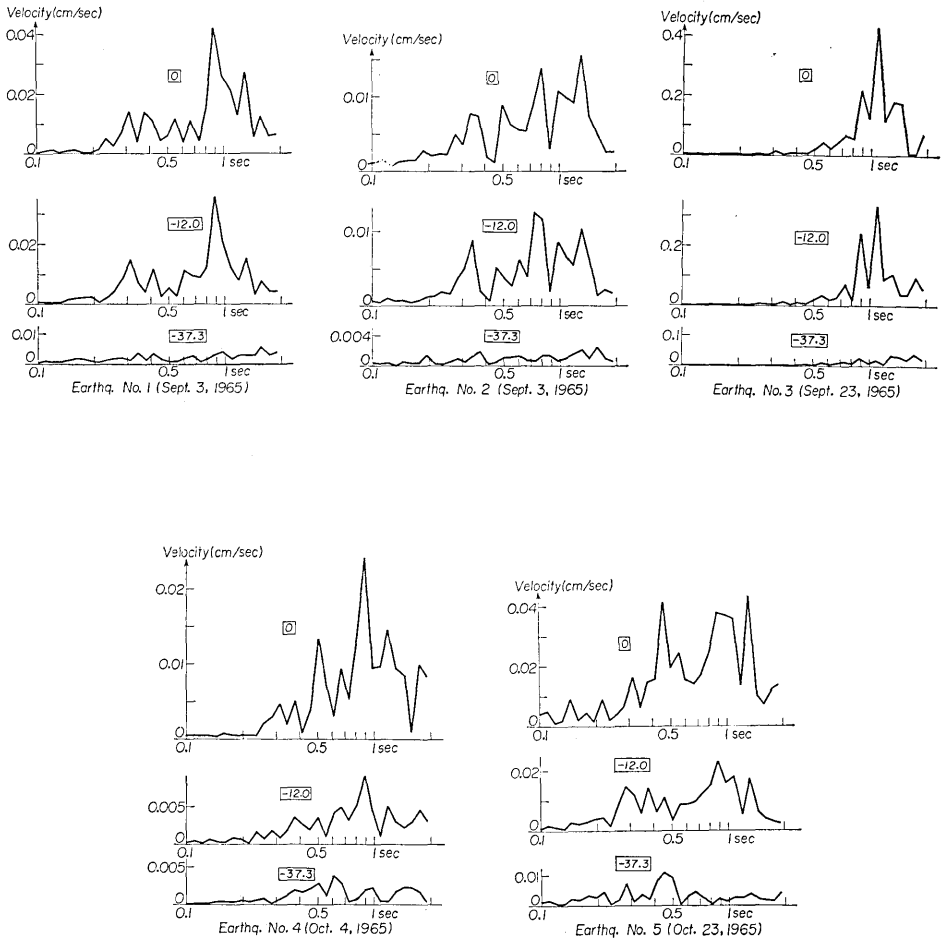

Fig. 31. Station Yokohama. Velocity spectra of the earthquake motions.

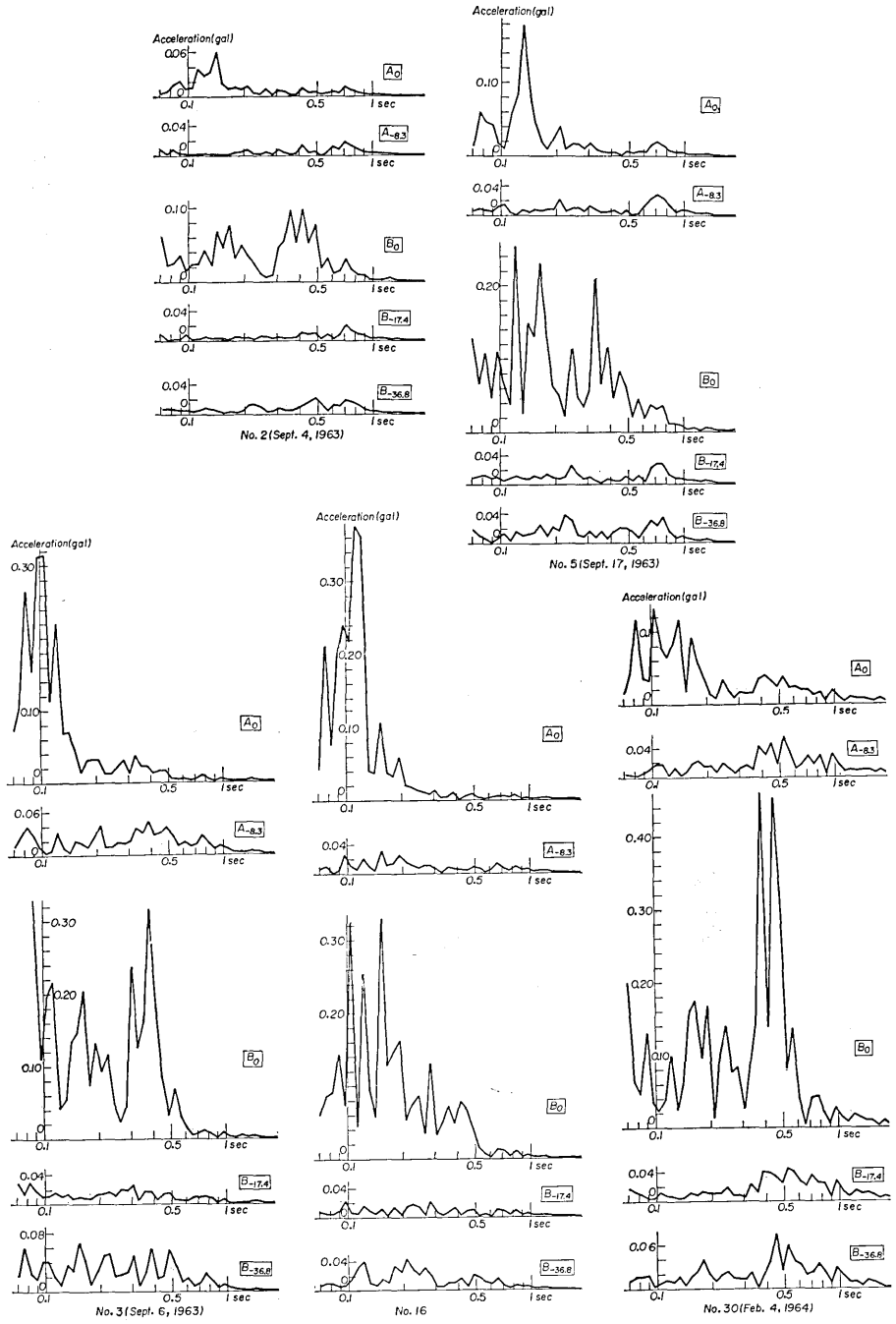

Fig. 32. Station Tsuruga. Acceleration spectra of the earthquake motions.

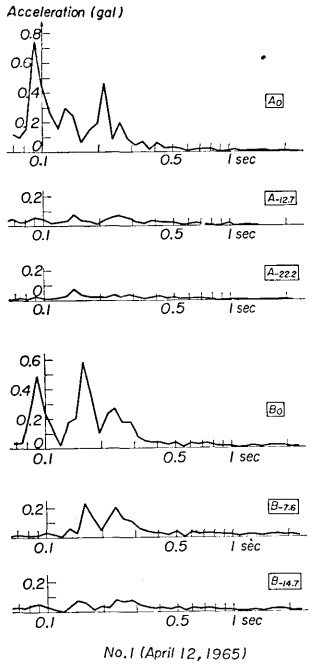

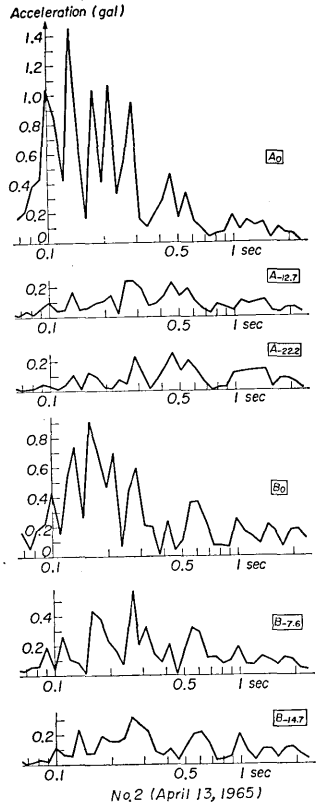

Fig. 33. Station Ōarai. Acceleration spectra of the earthquake motions.

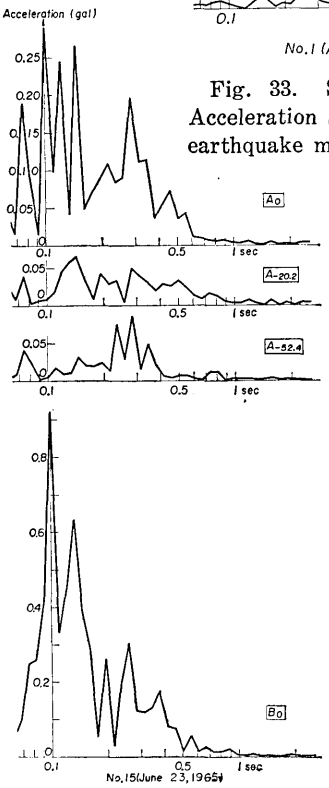

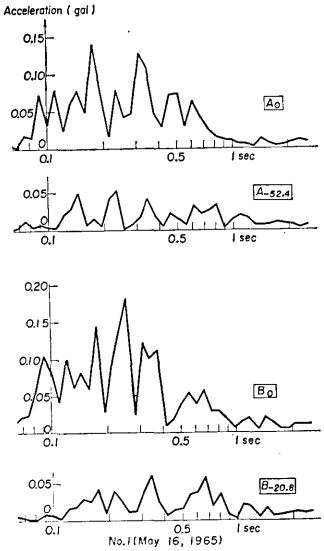

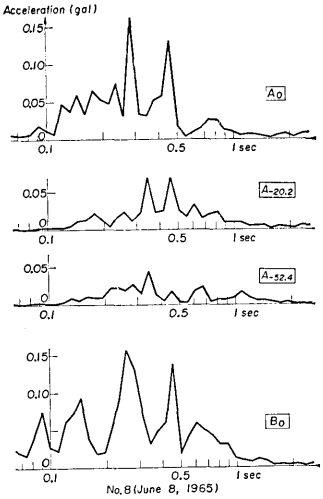

(to be continued)

(continued)

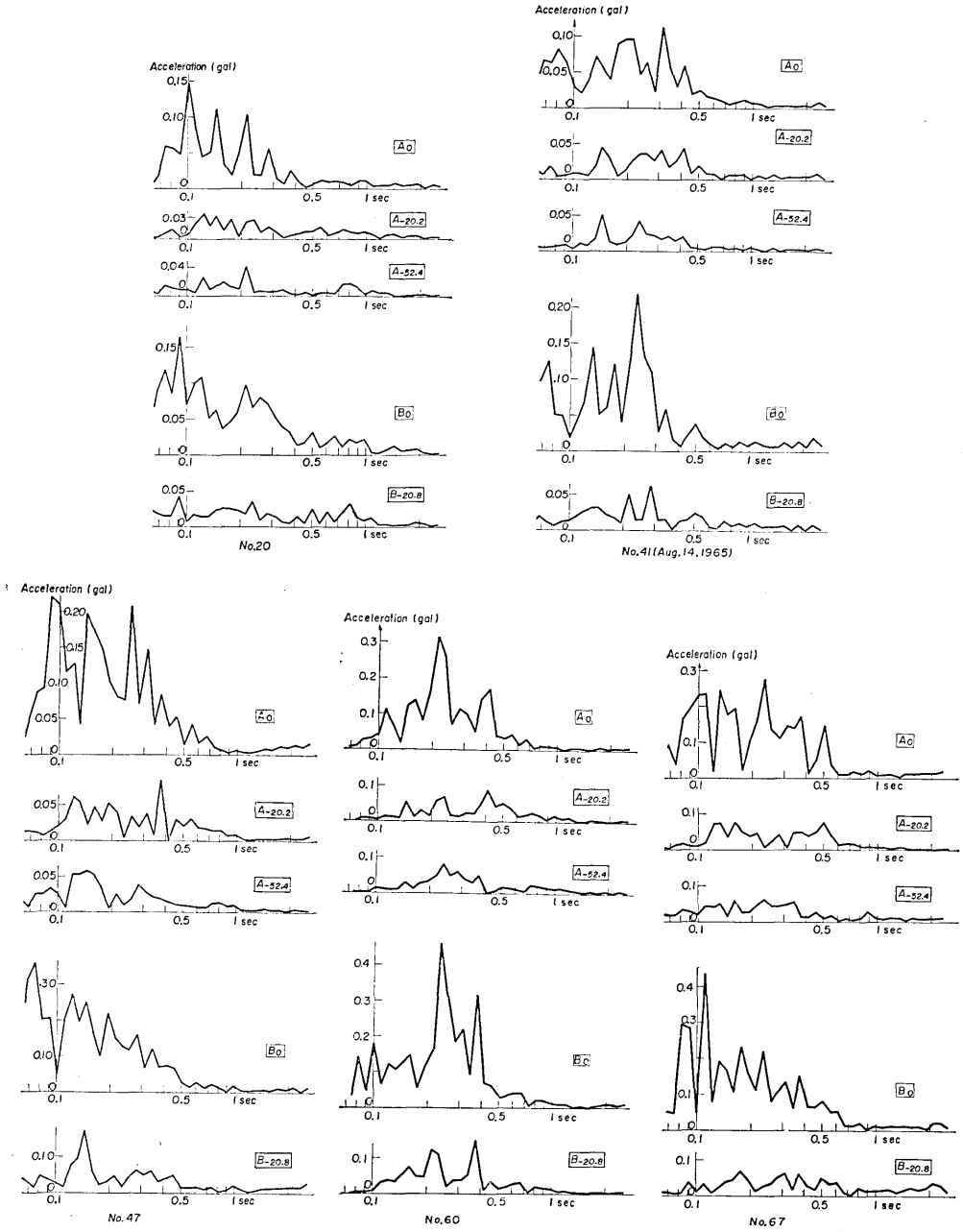

Fig. 34. Station Futaba. Acceleration spectra of the earthquake motions.

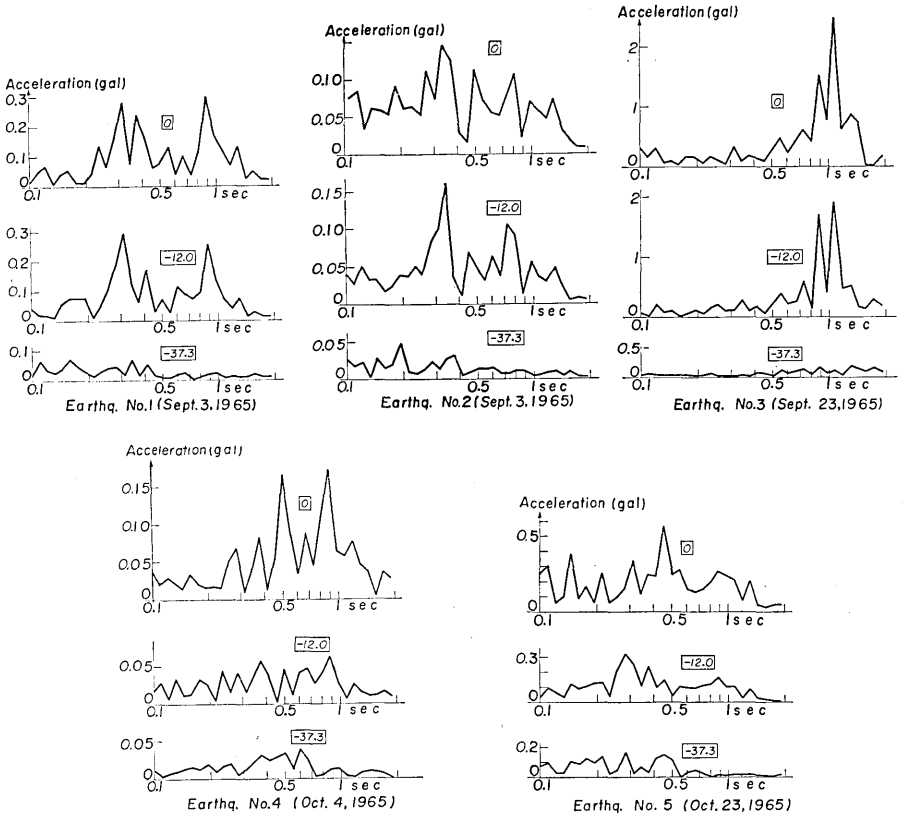

Fig. 35. Station Yokohama. Acceleration spectra of the earthquake motions.

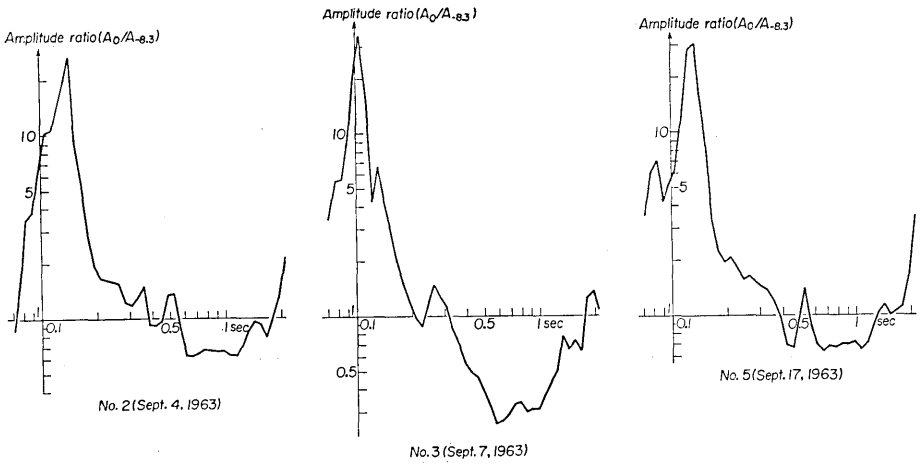

(to be continued)

(continued)

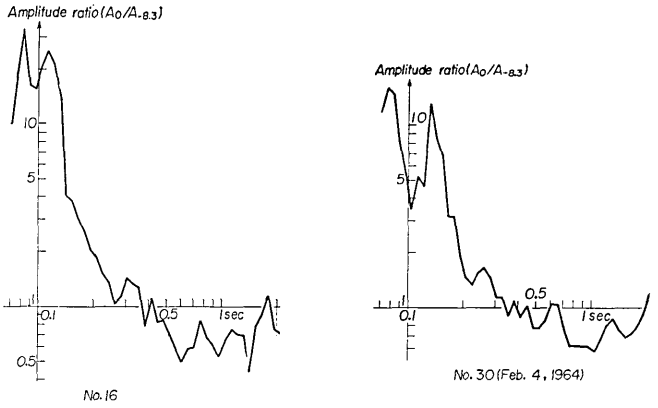

Fig. 36. Station Tsuruga A. Amplitude ratios between the surface and 8.3 m depth.

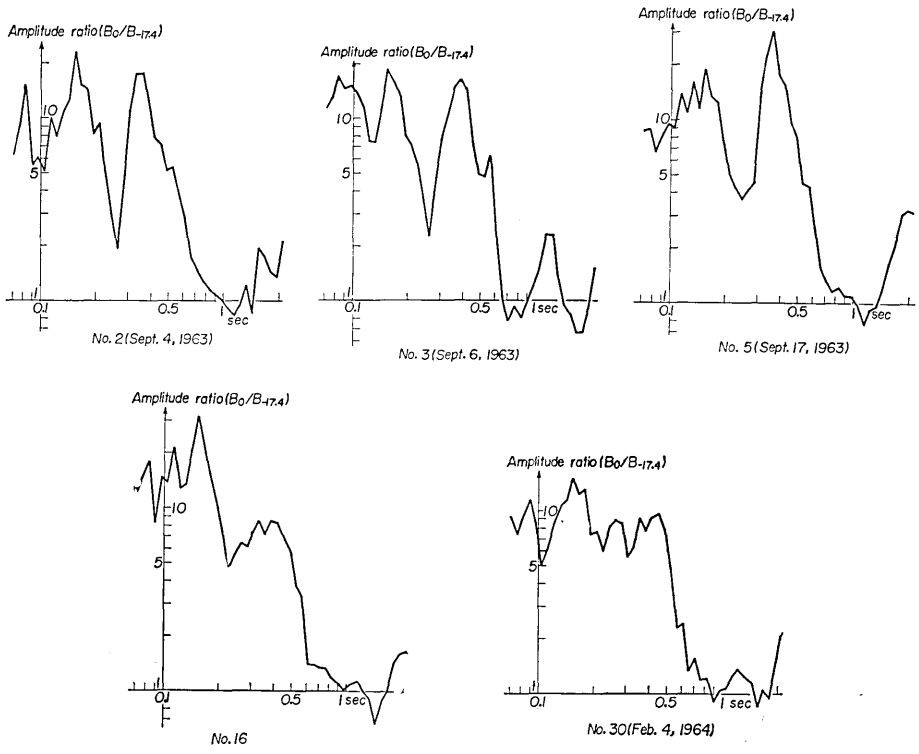

Fig. 37a. Station Tsuruga B. Amplitude ratios between the surface and 17.4 m depth.

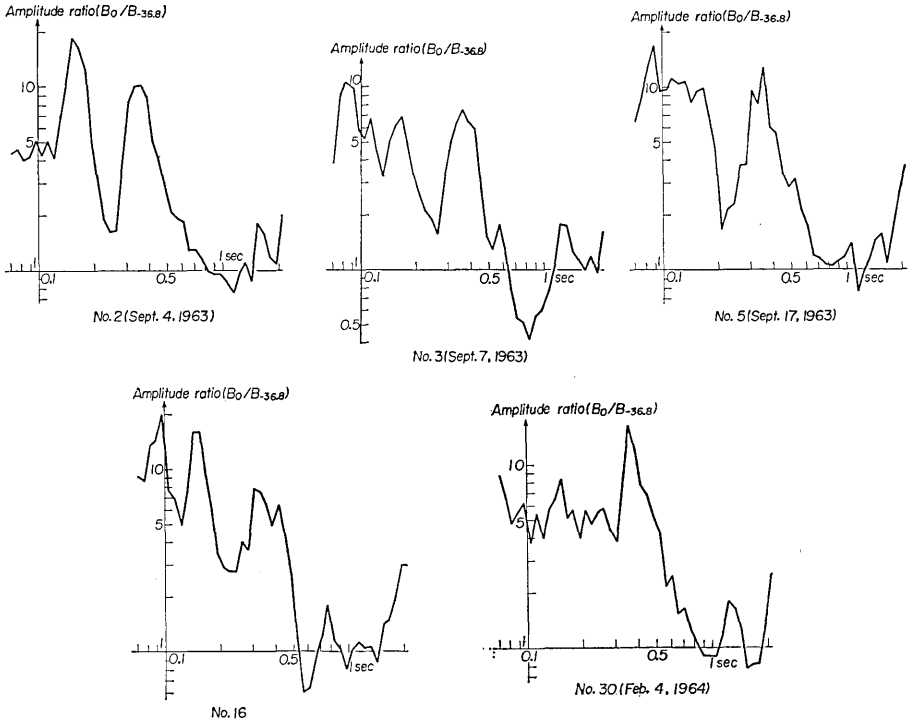

Fig. 37b. Station Tsuruga B. Amplitude ratios between the surface and 36.8 m depth.

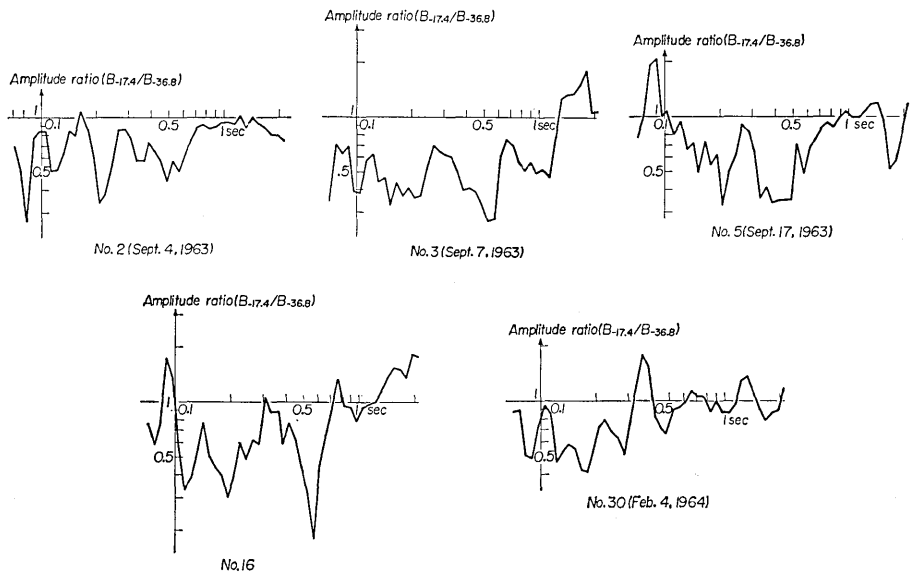

Fig. 37c. Station Tsuruga B. Amplitude ratios between 17.4 m depth and 36.8 m depth.

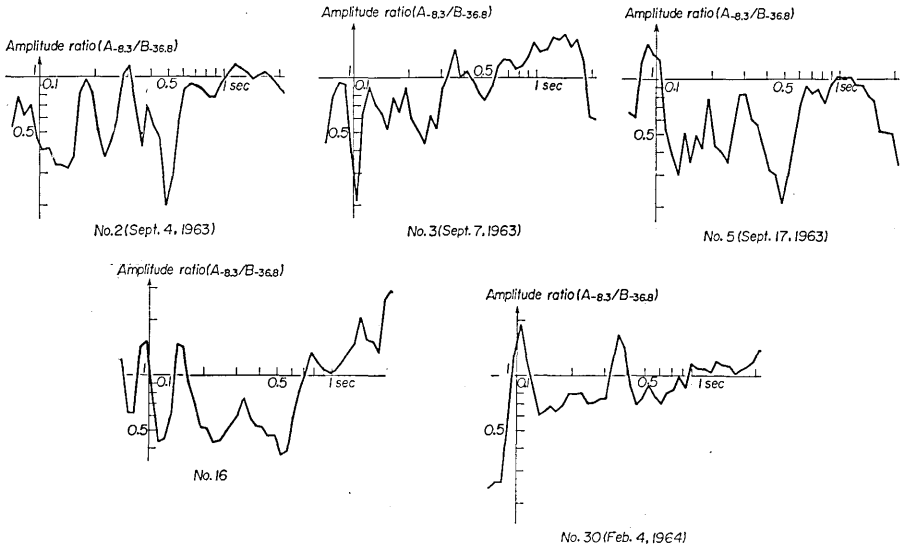

Fig. 38. Amplitude ratios between 8.3 m depth at A and 36.8 m depth at B of the station Tsuruga.

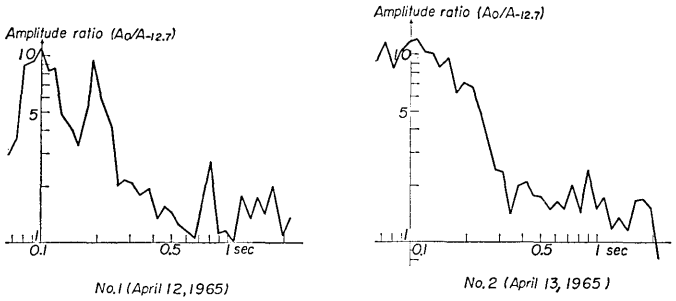

Fig. 39a. Station Ōarai A. Amplitude ratios between the surface and 12.7 m depth.

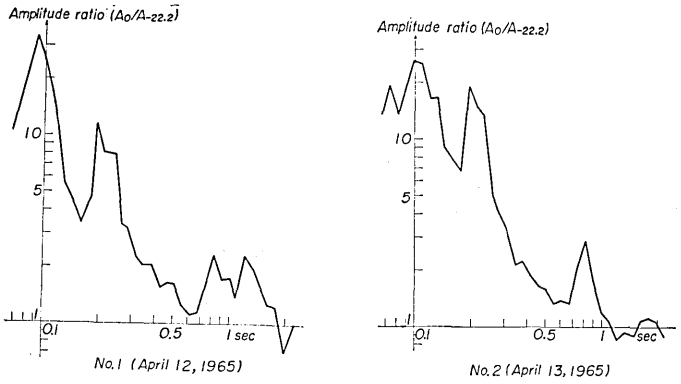

Fig. 39b. Station Ōarai A. Amplitude ratios between the surface and 22.2 m depth.

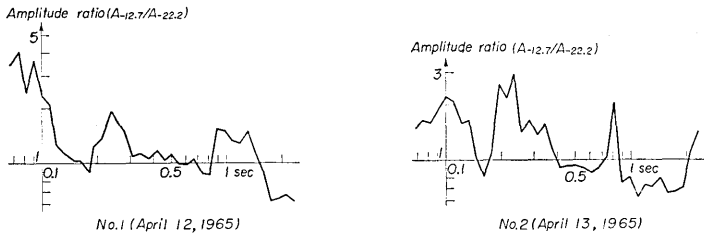

Fig. 39c. Station Ōarai A. Amplitude ratios between 12.7 m depth and 2.22 m depth.

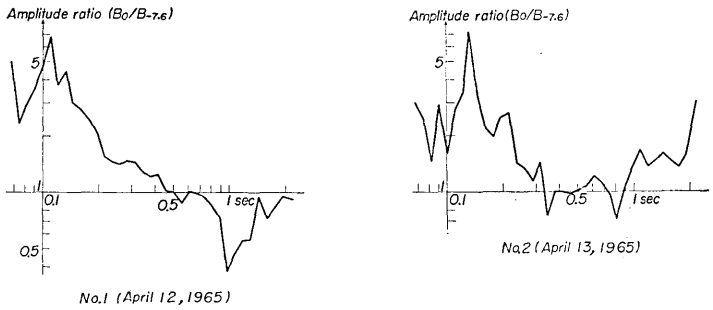

Fig. 40a. Station Ōarai B. Amplitude ratios between surface and the 7.6 m depth.

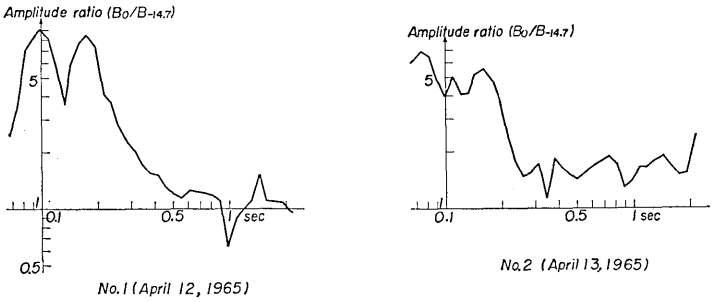

Fig. 40b. Station Ōarai B. Amplitude ratios between the surface and 14.7 m depth.

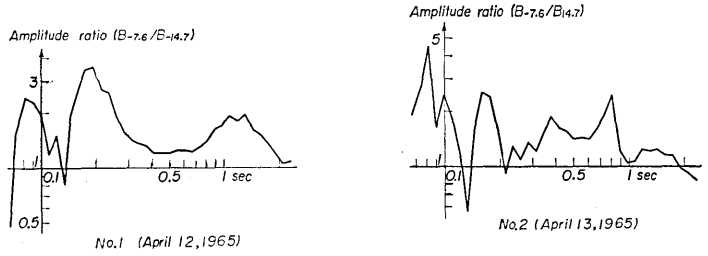

Fig. 40c. Station Ōarai B. Amplitude ratios between 7.6 m depth and 14.7 m depth.

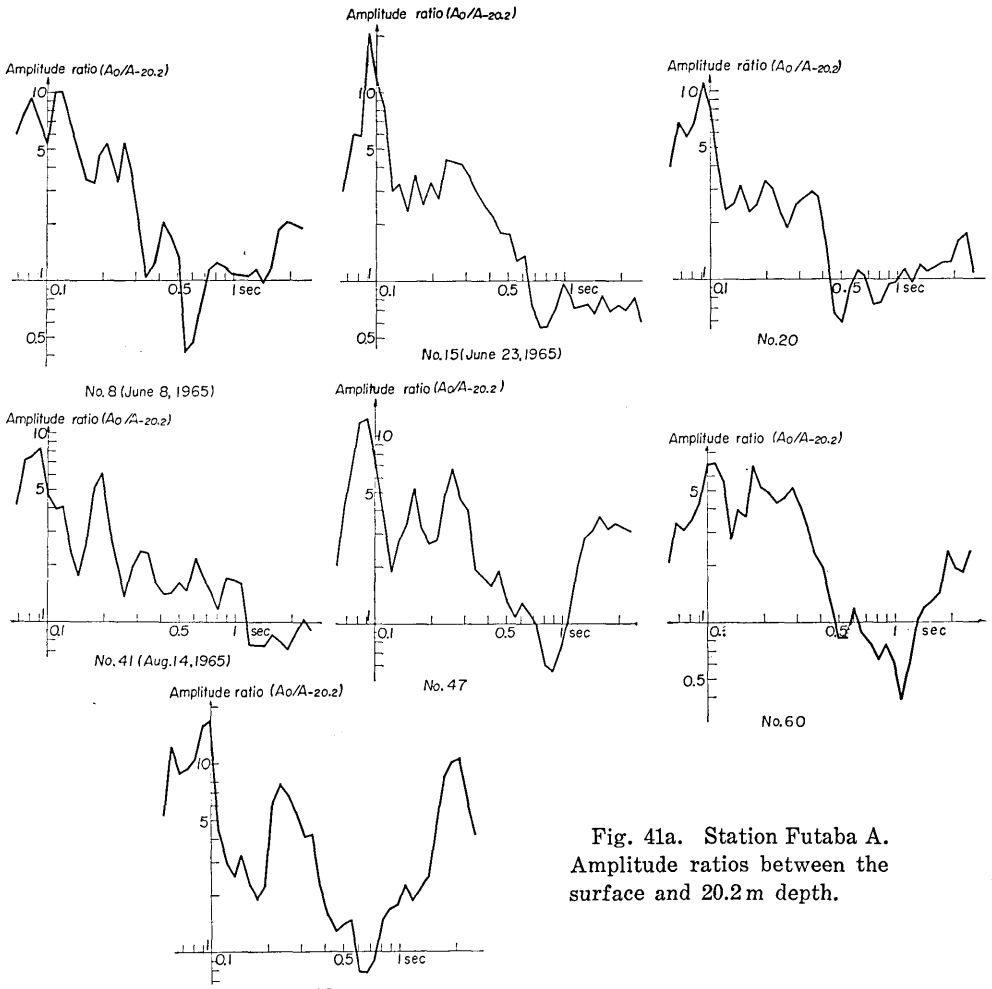

Fig. 41a. Station Futaba A. Amplitude ratios between the surface and 20.2 m depth.

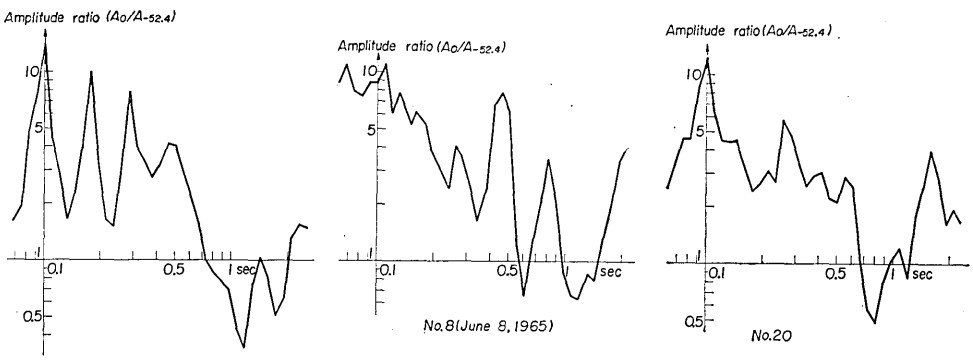

(to be continued)

(continued)

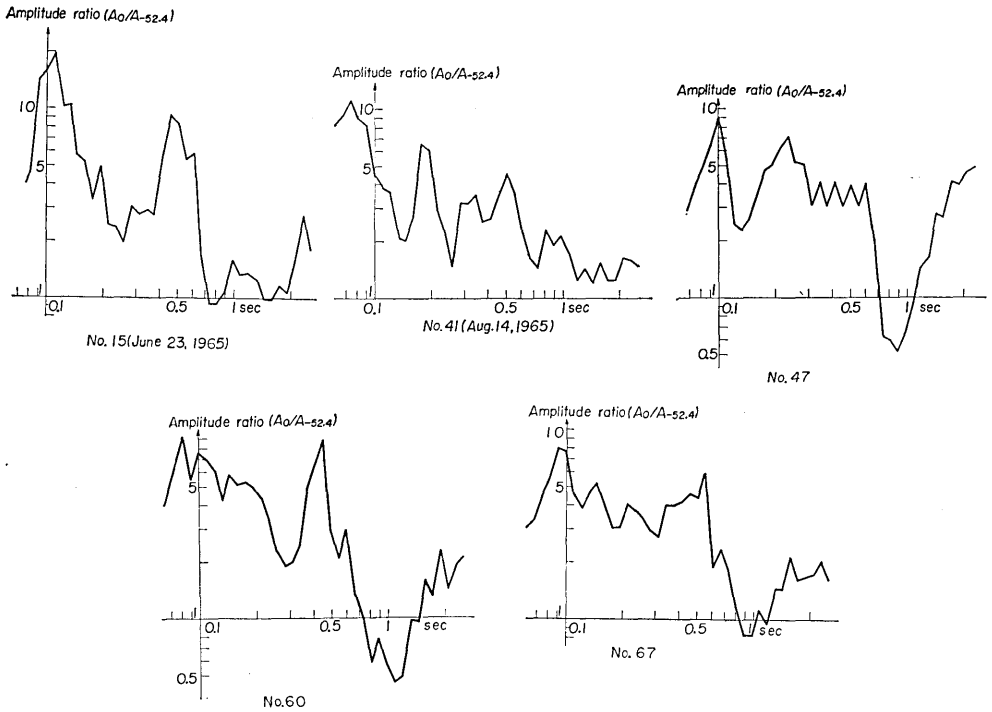

Fig. 41b. Station Futaba A. Amplitude ratios between the surface and 52.4 m depth.

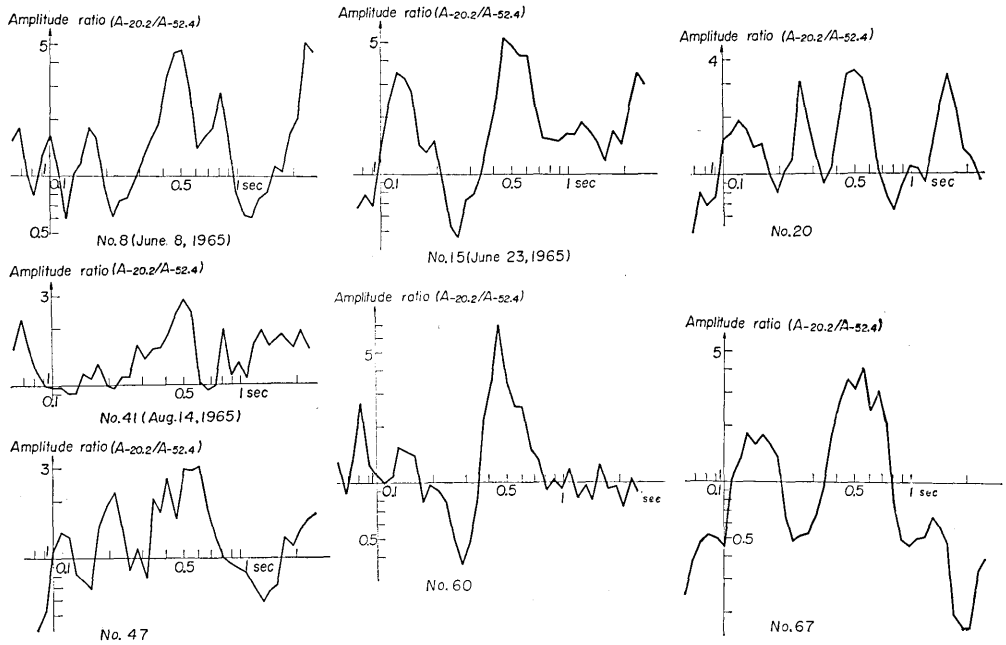

Fig. 41c. Station Futaba A. Amplitude ratios between 20.2 m depth and 52.4 m depth.

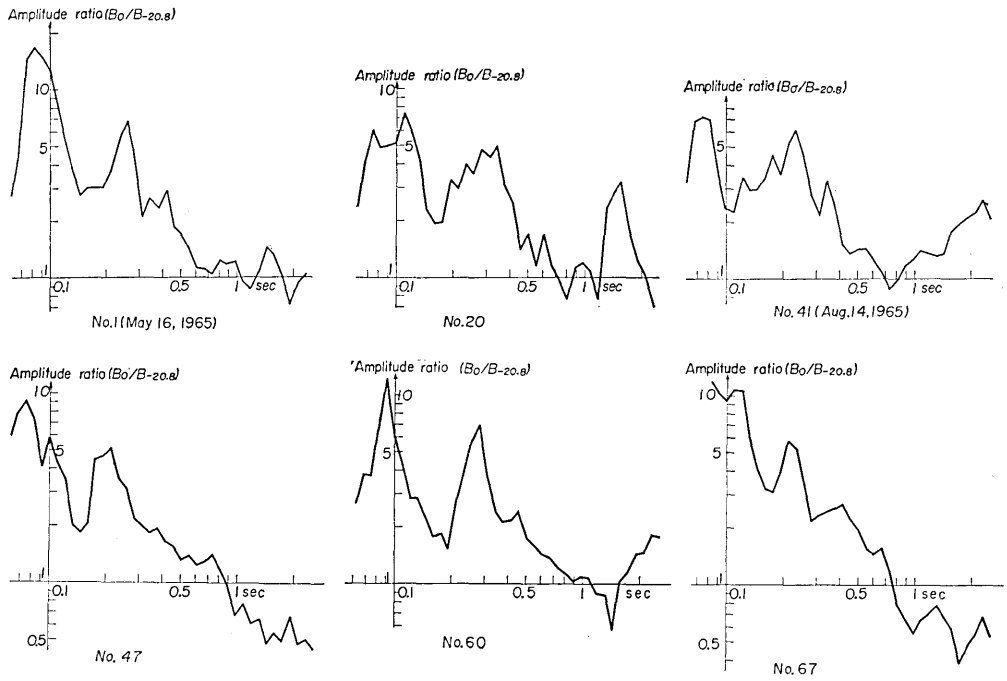

Fig. 42. Station Futaba B. Amplitude ratios between the surface and 20.8 m depth.

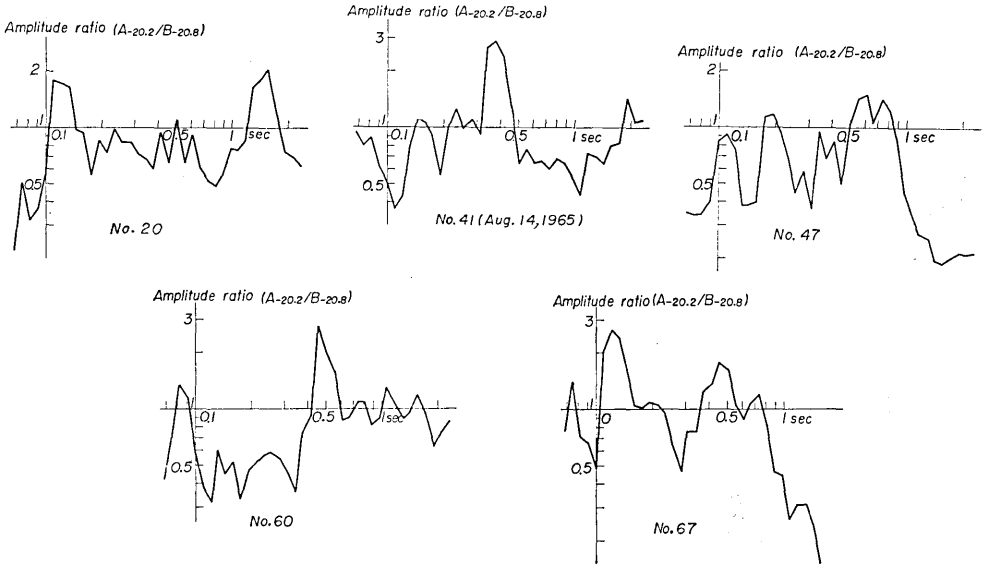

Fig. 43. Amplitude ratios between 20.2 m depth at A and 20.8 m depth at B of the station Futaba.

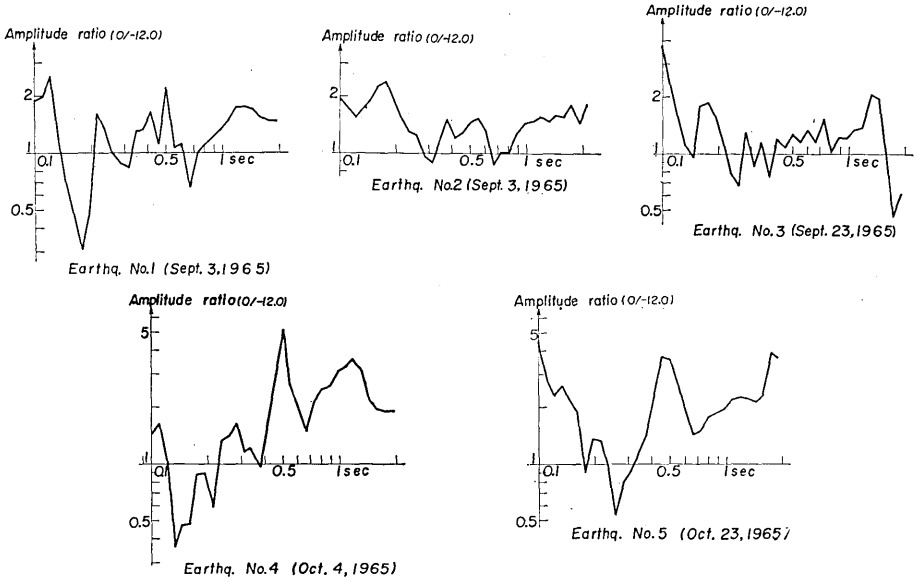

Fig. 44a. Station Yokohama. Amplitude ratios between the surface and 12.0 m depth.

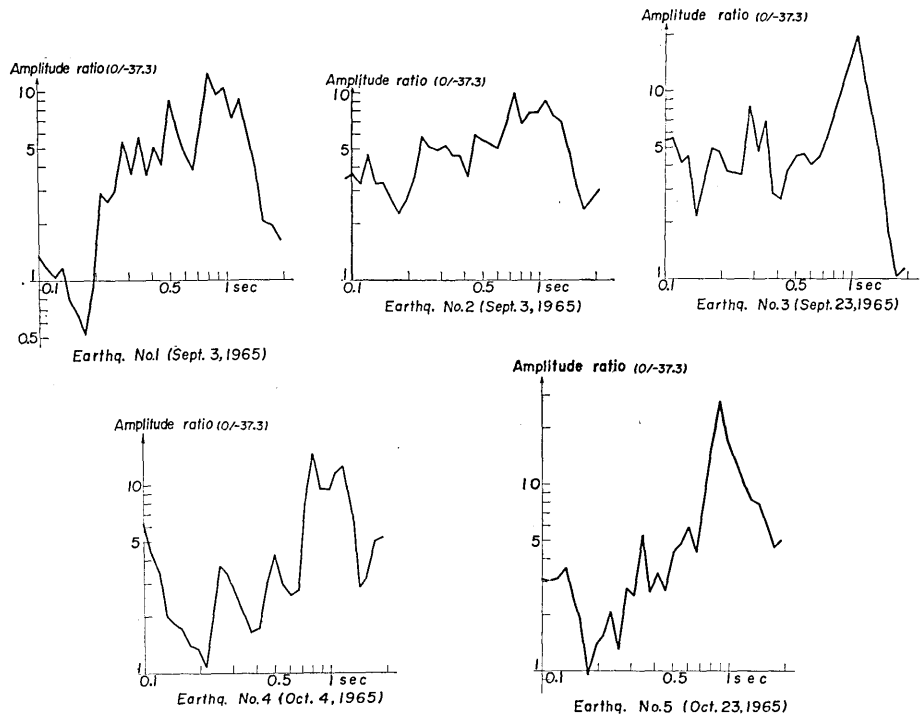

Fig. 44b. Station Yokohama. Amplitude ratios between the surface and 37.3 m depth.

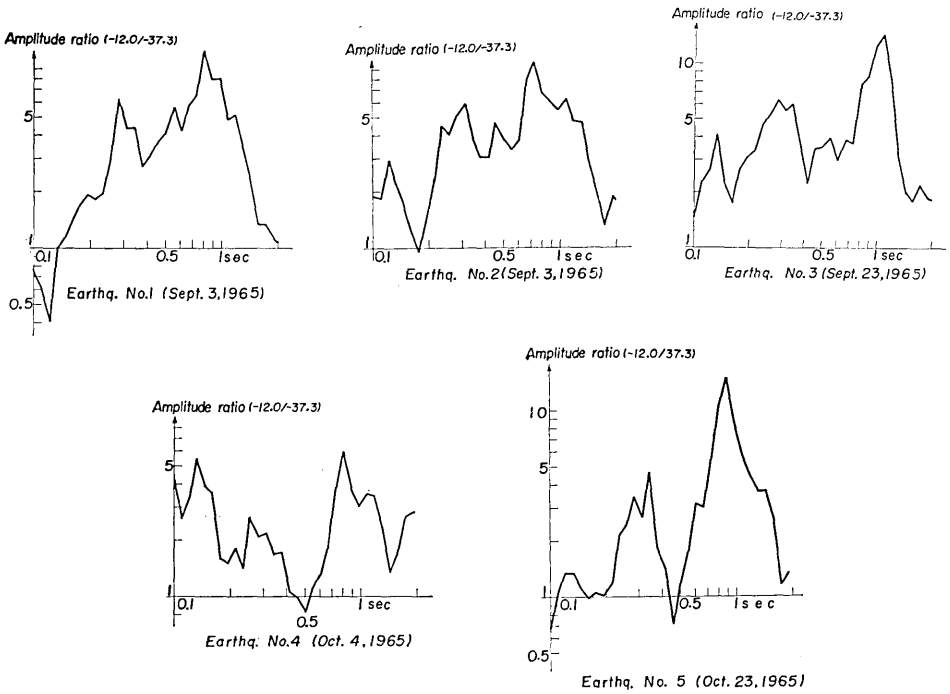

Fig. 44c. Station Yokohama. Amplitude ratios between 12.0 m depth and 37.3 m depth.

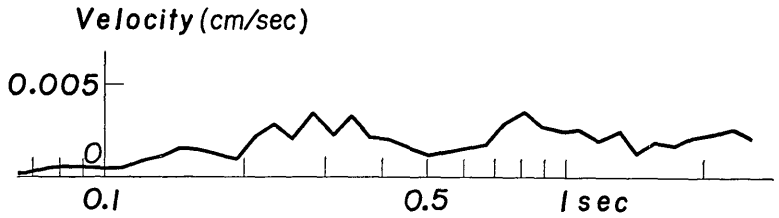

Fig. 45. Average curve of the velocity spectra of the earthquakes observed at the depth of 52.4 m of the station Futaba.

35. 地下における地震動の研究　第2報

地震研究所　金井　清／田中貞二／吉沢静代／森下利三／長田甲斐男／鈴木富三郎

深さのちがう 3 点での地震動の同時観測の結果から，近地地震の卓越振動部分の性質は，地盤内での重複反射の現象に支配されるということが，一層よく確められた．また，地中における地震動の速度振幅の観測結果から，基盤における地震動スペクトルに関する実験式 (5) が，地震工学上に利用価値のあることも，よくわかつた．